Conservation of Bacterial Protein Synthesis Machinery: Initiation and Elongation in *Mycobacterium smegmatis*[†]

Christian M. Bruell,[‡,§] Carolin Eichholz,[‡,||,⊥] Andriy Kubarenko,[||,#] Virginia Post,[§,○] Vladimir I. Katunin,[▽] Sven N. Hobbie,[§] Marina V. Rodnina,*[,||,⊥] and Erik C. Böttger*[,§]

Institute of Medical Microbiology, University of Zurich, Gloriastrasse 32, CH-8006 Zurich, Switzerland, Institute of Physical Biochemistry, University of Witten/Herdecke, Stockumer Strasse 10, 58448 Witten, Germany, Department of Physical Biochemistry, Max Planck Institute for Biophysical Chemistry, 37077 Goettingen, Germany, and Petersburg Nuclear Physics Institute, Russian Academy of Science, 188300 Gatchina, Russia

Received March 27, 2008; Revised Manuscript Received June 28, 2008

ABSTRACT: Most of our understanding of ribosome function is based on experiments utilizing translational components from *Escherichia coli*. It is not clear to which extent the details of translation mechanisms derived from this single organism are true for all bacteria. Here we investigate translation factor-dependent reactions of initiation and elongation in a reconstituted translation system from a Gram-positive bacterium *Mycobacterium smegmatis*. This organism was chosen because mutations in rRNA have very different phenotypes in *E. coli* and *M. smegmatis*, and the docking site for translational GTPases, the L12 stalk, is extended in the ribosomes from *M. smegmatis* compared to *E. coli. M. smegmatis* genes coding for IF1, IF2, IF3, EF-G, and EF-Tu were identified by sequence alignments; the respective recombinant proteins were prepared and studied in a variety of biochemical and biophysical assays with *M. smegmatis* ribosomes. We found that the activities of initiation and elongation factors and the rates of elemental reactions of initiation and elongation of protein synthesis are remarkably similar with *M. smegmatis* and *E. coli* components. The data suggest a very high degree of conservation of basic translation mechanisms, probably due to coevolution of the ribosome components and translation factors. This work establishes the reconstituted translation system from individual purified *M. smegmatis* components as an alternative to that from *E. coli* to study the mechanisms of translation and to test the action of antibiotics against Gram-positive bacteria.

Synthesis of proteins on the ribosome comprises four distinct steps: initiation, elongation, termination, and ribosome recycling. In bacteria, initiation entails a series of elemental steps in which three initiation factors (IF),[1] IF1, IF2, and IF3, are involved. In the first step, the small ribosomal subunit (30S) binds mRNA, the initiator tRNA (fMet-tRNA^{fMet}), and the three initiation factors, forming the 30S initiation complex (30S IC). Upon joining of the 30S IC with the large ribosomal subunit (50S), the IFs dissociate from the 70S IC bearing fMet-tRNA^{fMet} at the P site, to which an elongator aminoacyl-tRNA (aa-tRNA) can bind to the corresponding mRNA codon in the A site (*1*). Aa-tRNA is delivered to the ribosome in a complex with elongation factor Tu (EF-Tu) and GTP. After aa-tRNA is accommodated in the A site, peptide bond formation takes place, which is catalyzed by the ribosome itself and does not require accessory factors. Directional movement of tRNA and mRNA on the ribosome is catalyzed by elongation factor G (EF-G) under consumption of GTP. Protein synthesis is terminated when the ribosome encounters a stop codon. During termination, peptidyl-tRNA is hydrolyzed by the ribosome aided by release factors, and the peptide is released from the ribosome. Finally, ribosomes are split into subunits, and the deacylated tRNA is released by a combined action of EF-G and ribosome release factor (RRF) aided by IF3 (*2–4*).

Several components, e.g., rRNA (rRNA), ribosomal proteins, aa-tRNA, and translation factors, are involved in positioning, catalysis, and movement of the substrates during translation, and their functionally important domains are highly conserved, implying that translation must function in very much the same way in all bacteria. In fact, sequence alignments of rRNA and translation factors reveal a high degree of conservation in core structural elements that are most important for catalytic functions (*5, 6*). However, the

[†] This work was supported by grants of the Bonizzi-Theler Stiftung (to E.C.B. and S.N.H.), the Deutsche Forschungsgemeinschaft (to M.V.R.), the Russian Foundation for Basic Research (to V.I.K.), and the International Bureau of the Federal Ministry of Education and Research, Germany (to M.V.R. and V.I.K.).

* Corresponding authors. E.C.B.: e-mail, boettger@immv.uzh.ch; tel, 41 44634 2660; fax, 41 4463 44906. M.V.R.: e-mail, rodnina@uni-wh.de; tel, 49 2302 926117; fax, 49 2302 926205.

[‡] These authors contributed equally to the work.

[§] University of Zurich.

[||] University of Witten/Herdecke.

[⊥] Max Planck Institute for Biophysical Chemistry.

[#] Current affiliation: German Cancer Research Center, Im Neuenheimer Feld 242, 69120 Heidelberg, Germany.

[○] Current affiliation: School of Molecular and Microbial Biosciences, The University of Sydney, Sydney, New South Wales 2006, Australia.

[▽] Russian Academy of Science.

[1] Abbreviations: mant-GDP, 2′(3′)-*O*-(*N*-methylanthraniloyl)guanosine 5′-diphosphate; mant-GTP, 2′(3′)-*O*-(*N*-methylanthraniloyl)guanosine 5′-triphosphate; IF, initiation factor; EF, elongation factor; aa-tRNA, aminoacyl-tRNA.

10.1021/bi800527k CCC: $40.75
Published on Web 08/02/2008

Table 1: mRNA Constructs[a]

name	nucleotide sequence (5′ to 3′ end)	features
MFTI-mRNA	GGCAA*GGAGG*UAAAUAAUGUUCACGAUC	SD-AUG-F-T-I
AUG-$(UUU)_{12}$	GCGGCAA*GGAGG*UAAAUAAUG$(UUU)_{12}$**UAA**GCAGG	SD-AUG-F_{12}-stop
AUU-$(UUU)_{12}$	GCGGCAA*GGAGG*UAAAUAAUU$(UUU)_{12}$**UAA**GCAGG	SD-AUU-F_{12}-stop
poly(U)	$(UUU)_n$	F_n

[a] The Shine−Dalgarno (SD) sequences are shown in italics, the start codons are underlined, and the stop codons are in bold (F = phenylalanine, T = threonine, and I = isoleucine). Poly(U) had an average length of 180 nucleotides ($n = 60$) (calculated from manufacturer's data).

evolutionary pressure to adapt to diverse environments also caused diversifications in sequences of rRNA and protein factors involved in translation (*7*). When studying the effects of mutations in catalytic centers of the ribosome, significant species-specific differences were observed, e.g., with respect to viability of defined rRNA mutations in the peptidyl transferase center on the 50S subunit, G2447U and A2451U in 23S rRNA (*8–11*), as well as in the decoding site on the 30S subunit, e.g., U1406 and U1495 (*12–15*). Another notable difference between the ribosomes from different species concerns the composition of the L12 stalk, which is the interaction site for translational GTPases, including IF2, EF-Tu, and EF-G. While in *E. coli* the L12 stalk contain four copies of ribosomal protein L12, a number of other bacteria appear to have six copies of the protein (*16–18*). Protein L12 is essential for rapid docking of factors to the ribosome and GTPase activation (*17*); however, the importance of the extended L12 stalk is not known.

Structural information on the translational machinery is available for a number of different organisms such as *E. coli* (*Eco*), *Haloarcula marismortui, Thermus thermophilus, and Deinococcus radiodurans* (*19–24*). However, for biochemical and genetic studies, mostly *E. coli* translation components have long been used. This is because all purified components required for such studies, particularly ribosomal subunits and translation factors, are available from *Eco* and because *Eco* is a standard model organism for genetic manipulation. So far, very little is known about translation in other bacteria (*1, 25–28*). *M. smegmatis* (*Msm*) is a Gram-positive eubacterium which has been established as a versatile genetic model for rRNA mutagenesis (*29–31*). Establishing translation assays reconstituted from purified *Msm* components would provide the compelling possibility not only to validate the functional models of protein synthesis but also to study mutant ribosomes in more detail (*31–33*).

In this study we addressed the question of whether and to which degree the mechanisms of translation initiation and elongation are conserved between *Msm* and *Eco*, which belong to different bacterial phyla, i.e., Gram-positive and Gram-negative microorganisms, and appear to have six and four copies of ribosomal protein L12, respectively (*16*). We prepared recombinant initiation and elongation factors from *M. smegmatis* and developed a reconstituted translation system which utilizes purified ribosomes, initiation and elongation factors from *M. smegmatis*. The activities of factors from *E. coli* and *M. smegmatis* were investigated and the thermodynamic and kinetic constants of the key elemental reactions of initiation and translation compared.

MATERIALS AND METHODS

Chemicals and Buffers. Chemicals for cloning, expression, and purification of translation factors, for ribosome isolation and activity assays, were purchased from Merck (Darmstadt, Germany), Sigma-Aldrich (Buchs, Switzerland), Fluka (Buchs, Switzerland), ACROS Organics (Geel, Belgium), or AppliChem (Darmstadt, Germany). Champion pET Directional TOPO expression kit was from Invitrogen (Carlsbad, CA).

Buffer A: 50 mM Tris-HCl, pH 7.5, 70 mM NH_4Cl, 30 mM KCl, and 7 mM $MgCl_2$. Buffer B: 20 mM sodium phosphate, pH 7.4, and 0.5 M NaCl. Buffer C: 20 mM sodium phosphate, pH 7.4, 0.5 M NaCl, and 0.5 M imidazole. MFTI-mRNA (Table 1) was purchased from Dharmacon Research, Inc. (Boulder, CO), AUG$(UUU)_{12}$-mRNA and AUU-$(UUU)_{12}$-mRNA were from Microsynth AG (Balgach, Switzerland), and poly(U) was from Amersham Biosciences (Otelfingen, Switzerland). Fluorescein-labeled mRNA was purchased from CureVac GmbH (Tuebingen, Germany). Mant nucleotides were purchased from Jena Bioscience (Jena, Germany). f[^{3}H]Met-tRNA^{fMet} was prepared according to ref *34*. Ribosomes, translation factors, and tRNA^{Phe} from *E. coli* were prepared as described (*35, 36*).

Identification, Cloning, Expression, and Purification of Translation Factors. Genomic DNA was isolated from *M. smegmatis* strain mc^{2}155 and used as template for amplification of the genes coding for translation initiation and elongation factors by PCR. PCR primers were designed such that a CACC recognition site was added upstream of the 5′-end of the coding sequence that enabled directional cloning using a topoisomerase kit. The successful amplification of GC-rich genomic DNA templates required the addition of up to 8% of DMSO and optimized annealing temperatures. All genes were cloned into the pET100 and pET101 expression vector system (Champion pET Directional TOPO expression kits; Invitrogen) and controlled for the absence of mutations by DNA sequencing.

The competent *E. coli* strain BL21 Star (DE3) was transformed with plasmid DNA of pET100 or pET101 vector constructs harboring the genes of initiation and elongation factors. All factors that were used in this study carried an N-terminal tag consisting of 36 additional amino acids including six histidines and an enterokinase recognition site. Overexpression of recombinant proteins was induced by addition of isopropyl β-D-1-thiogalactopyronoside (IPTG) (0.5 mM) to cultures growing at midlog phase in Luria−Bertani (LB) media with carbenicillin (50 μg/mL). After 2−4 h of expression, cells were harvested by centrifugation with 10000*g* for 10 min. All centrifugation steps were performed at 4 °C. Pellets were washed with buffer B, shock frozen, and stored at −80 °C until protein purification.

To purify the proteins by affinity chromatography, cells were resuspended in buffer B and opened by two passages through a French pressure cell (American Instrument Co., MD) at 16000 psi. The cell lysate was incubated with DNase (RQ RNase free DNase; Promega, Madison, WI) for 10 min

on ice, and cell debris was separated by centrifugation for 30 min at 30000*g*. For affinity chromatography a HisTrap HP column (Amersham Biosciences, Uppsala, Sweden), equilibrated in buffer B, was loaded with lysate filtered through 0.8 μm syringe filter. The column was washed with buffer B and $(His)_6$-tagged proteins eluted by a gradient from buffer B to 100% buffer C. Fractions containing protein were identified by absorption at 280 nm, pooled, and dialyzed against buffer A. Preparations were concentrated with Vivaspin 6 concentrators (Sartorius, Goettingen, Germany), supplemented with 15% glycerol, quick-frozen in liquid nitrogen, and stored at −80 °C.

Isolation of 70S Ribosomes and Ribosomal Subunits from M. smegmatis. Cells of *M. smegmatis* mc^2155 were grown to the logarithmic growth phase in LB medium with 0.05% Tween 80 at 37 °C. Out of 20 L of culture media 24−28 g of wet cell pellet was harvested by centrifugation at 10000*g* for 10 min, quick-frozen, and stored at −80 °C. Details of isolation of 70S ribosomes are described elsewhere (*32*). Ribosomal subunits were obtained from purified 70S ribosomes by dissociation at low Mg^{2+} conditions (buffer A with 1 mM $MgCl_2$) and separated by centrifugation through 10−40% sucrose gradients in swing-out buckets (Beckman, SW28) for 16 h at 110000*g* (25000 rpm). Complete dissociation of 70S ribosomes was achieved at these conditions. The fractions containing 30S and 50S subunits were pooled and subunits pelleted by centrifugation for 20 h at 300000*g* in a fixed-angle rotor (Beckman, Ti50.2). 50S and 30S subunits were resuspended in buffer A, frozen in liquid nitrogen, and stored at −80 °C. The concentration of ribosomes was estimated by measuring absorbance at 260 nm assuming that 1 A_{260} corresponds to 23 pmol of 70S ribosomes, 37 pmol of 50S subunits, or 67 pmol of 30S subunits.

30S and 70S Initiation Complex Formation. 70S initiation complex was formed using 70S ribosomes (0.5 μM), MFTI-mRNA (1 μM), f[^{3}H]Met-tRNA^{fMet} (1 μM; specific activity 3000−3500 dpm/pmol), initiation factors (1 μM, if not stated otherwise), and GTP (1 mM) for 60 min (if not indicated otherwise) at 37 °C in buffer A or in the absence of the factors (phasing) with 70S ribosomes (3 μM), fMet-tRNA^{fMet} (4.5 μM), MFTI-mRNA (4.5 μM), and DTT (3 mM) in buffer A with 20 mM Mg^{2+} for 15 min at 37 °C. Initiation complexes were isolated by nitrocellulose filtration (0.45 μm pore size; Sartorius, Goettingen, Germany). Filters were dissolved in 10 mL of scintillation cocktail (Quickscint 361; Zinsser Analytic, Frankfurt, Germany), and radioactivity was quantified by liquid scintillation counting.

To form 30S initiation complexes, 30S subunits (0.25 μM) were incubated with f[^{3}H]Met-tRNA^{fMet} (0.5 μM), MFTI-mRNA (0.5 μM), and GTP (1 mM) in buffer A for 1 min at 37 °C. Binding of fMet-tRNA^{fMet} to 30S subunits was measured with increasing amounts of either IF2 or IF1 in the presence of a constant amount of IF2 (0.5 μM). The reactions (6.25 pmol of 30S subunits) were stopped by addition of 1 mL of ice-cold buffer A, and complexes were isolated by nitrocellulose filtration and washed with 1 mL of ice-cold buffer A with 20 mM Mg^{2+}. Radioactivity was counted as described above.

Biochemical Assays. For translation assays, initiation complexes were formed by phasing on AUG-$(UUU)_{12}$ mRNA as described above. EF-Tu (8 μM) and EF-G (2 μM) were incubated in buffer A with GTP (4 mM), phosphoenolpyruvate (8 mM), and pyruvate kinase (0.2 mg/mL) for 15 min at 37 °C before [^{14}C]Phe-tRNA^{Phe} (6 μM, specific activity 800−900 dpm/pmol) was added. Initiation complexes (0.1 μM) were mixed with ternary complexes EF-Tu·GTP·[^{14}C]Phe-tRNA^{Phe} (3 μM) and EF-G (1 μM), and samples (2 pmol of 70S each) were taken at given time points (0.25−15 min). Reactions were stopped by addition of KOH (0.5 M), aa-tRNA hydrolyzed for 30 min at 37 °C, and peptides precipitated by addition of cold TCA (5%) and filtrated through nitrocellulose filters. Filters were dissolved in 10 mL of scintillation cocktail (Quickscint 361; Zinsser Analytic, Frankfurt, Germany), and radioactivity was quantified by liquid scintillation counting.

To study A-site binding, initiation complexes were prepared by phasing as described above, and Mg^{2+} concentration was adjusted to 7 mM. EF-Tu (amounts indicated in Figure 9a) was activated by incubating with GTP (3 mM), PEP (2 mM), and PK (0.1 mg/mL) for 15 min at 37 °C. After addition of [^{14}C]Phe-tRNA^{Phe} (0.24 μM) samples were incubated for 1 min at 20 °C to form ternary complexes. Initiation complexes (0.2 μM) were mixed with ternary complexes and incubated for 2 min at 20 °C. Samples were applied to nitrocellulose filters and washed with 3 mL of cold buffer A, and radioactivity was quantified.

To study multiple-turnover EF-G-dependent translocation, initiation complexes were prepared by phasing as described above, and Mg^{2+} concentration was adjusted to 14 mM. Ternary complexes were prepared as described above except for EF-Tu (1.2 μM) and [^{14}C]Phe-tRNA^{Phe} (0.9 μM) concentrations. Initiation complexes (0.5 μM) were mixed with equal volumes of ternary complexes (0.5 μM) yielding pretranslocation complexes. EF-G was activated by incubation in buffer A with 14 mM Mg^{2+} and GTP (5 mM) for 10 min at 37 °C. Multiple-turnover translocation was induced by addition of EF-G (0.5 nM) to pretranslocation complexes (0.2 μM). Translocation reaction was monitored by rapid reaction with Pmn (1 mM) for 10 s at 37 °C. The reaction was stopped by addition of 1.5 M NaOAc and saturated $MgSO_4$, pH 4.5, and fMetPhe-Pmn was extracted into ethyl acetate (*36*).

Rapid Kinetics. Experiments were performed on a SX-18MV stopped-flow apparatus from Applied Photophysics (Leatherhead, U.K.) equipped with a 150 W Xe short arc lamp. Time courses were taken using a logarithmic time base. Time courses shown are averages of 9−12 individual experiments.

Association of ribosomal subunits and dissociation of 70S ribosomes were monitored by changes in light scattering in buffer A at 37 °C. Light scattering was monitored at 436 nm, and the emission was detected unfiltered in a right angle to the excitation light beam. The rate constant of 30S and 50S association was calculated by numerical integration (MicroMath Scientist software) using the binding model 30S + 50S → 70S with known initial concentrations of subunits and assuming that the reverse reaction is close to zero (*34, 37*). Rate constants of 70S ribosome dissociation (70S → 30S + 50S) were estimated by single-exponential fitting using Graph Pad Prism 4 software.

Fluorescence changes of mRNA(Flu) or Phe-tRNA^{Phe}(Prf) upon translocation or A-site binding were monitored upon excitation at 470 nm, and the emission was detected after

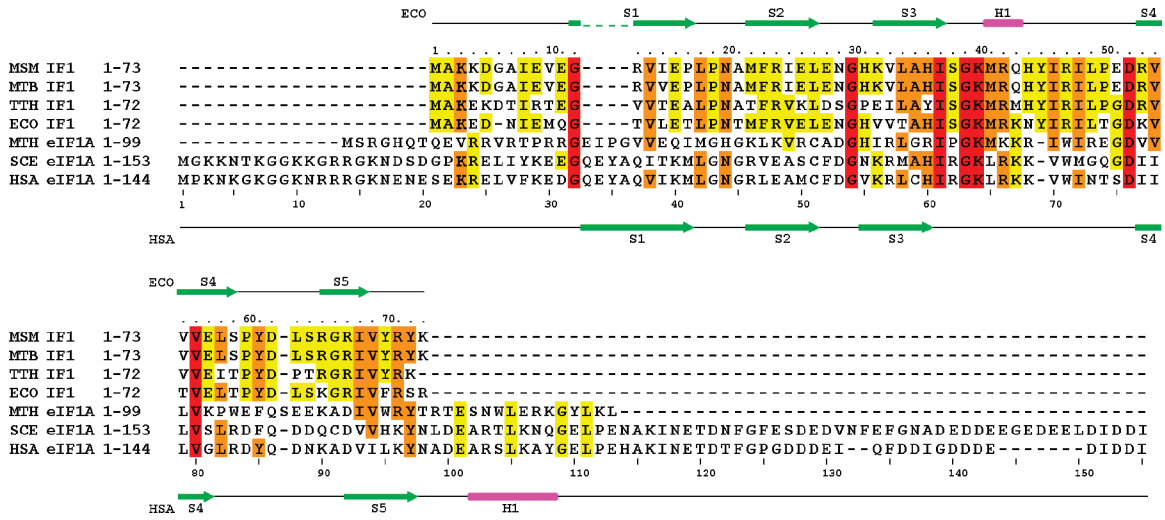

FIGURE 1: Sequence alignments of bacterial IF1 and eukaryotic eIF1A. Sequences are from MSM, *Mycobacterium smegmatis* (GenBank accession number (CP000480)); MTB, *Mycobacterium tuberculosis* (CAB08728.1); TTH, *Thermus thermophilus* (CAD42330); ECO, *Escherichia coli* (AAC73970.1); MTH, *Methanobacter thermautotropicus* (AAB85500.1); SCE, *Saccharomyces cerevisiae* (EDN62581); and HSA, *Homo sapiens* (NP001403). Sequence numbering on top corresponds to *M. smegmatis* and the numbering at the bottom to a continuous ruler. The secondary structure elements indicated at the top are from the structure of *Eco* IF1 (PDB entry 1ah9 (*39*)) and at the bottom from that of *H. sapiens* IF1A (PDB entry 1d7q (*74*)). The symbols are denoted as follows: α or 3_{10} helices, bars; β strands, arrows; unstructured regions, lines. Residues conserved in all proteins in sequence alignments are highlighted in red; those with sequence identity in the range of 70−85% and >40% are highlighted orange and yellow, respectively. Amino acid sequences were obtained from the NCBI database and aligned using Clustal (*75*).

passing a KV 500 cutoff filter (Schott, Mainz, Germany). For rapid kinetics experiments on A-site binding, EF-Tu·GTP·[^{14}C]Phe-tRNA^{Phe}(Prf) (0.1 μM) was purified by FPLC on a Superdex 75 column (*38*). Ternary complex (TC, 0.1 μM) and 70S initiation complex (IC, 0.3 μM) were rapidly mixed at 20 °C and fluorescence changes upon binding of TC to IC detected. Pretranslocation complexes were made of initiation complexes (0.25 μM) prepared by phasing on an mRNA(Flu) and purified ternary complexes (0.25 μM). Pretranslocation complexes (0.2 μM) and EF-G (2 μM) were rapidly mixed, and fluorescence change was detected.

Dissociation kinetics of mant nucleotides from EF-Tu and EF-G were monitored by FRET from Trp in the factors to the mant group. Fluorescence was excited at 290 nm and detected after passing a KV 408 cutoff filter (Schott, Mainz, Germany). EF-Tu·mant-GDP or mant-GTP complexes were prepared by incubation of EF-Tu·GDP (10 μM) with excess mant-GDP/GTP (100 μM) and purified from excess nucleotide on NAP10 (Pharmacia) gel filtration in buffer A. Phosphoenolpyruvate (3 mM) and pyruvate kinase (0.1 mg/mL) were added in the reaction mixture with mant-GTP. Dissociation of EF-Tu·mant-GDP (2 μM) was studied upon addition of excess nonmodified GDP (120 μM) in buffer A. Dissociation of EF-Tu·GTP (0.5 μM EF-Tu) was monitored upon addition of mant-GTP (25 μM). To measure dissociation of mant-GDP/GDP from EF-G, EF-G (1 μM) was preincubated with mant-GDP (8.5 μM) or mant-GTP (3.5 μM) and rapidly mixed with a solution containing unlabeled nucleotide (2.5 mM GDP; 1.2 mM GTP) in buffer A at 37 °C. Time courses were evaluated by exponential fitting with one (dissociation of mant nucleotides) or two (A-site decoding, translocation) exponential terms. In each case, the minimum number of exponential terms was used as required for a satisfactory fit; in each case fits with a smaller number of exponentials deviated significantly from the measured curves.

Steady-State Fluorescence Measurements. Fluorescence titrations were performed on a PTI spectrofluorometer (Photon Technology International; Birmingham, NJ) with a 75 W xenon arc lamp as light source. FRET from Trp to mant was measured after excitation at 290 nm and emission at 445 nm (mant) upon addition to EF-G of increasing concentrations of mant nucleotide. The values obtained in parallel for the same amounts of mant nucleotide in the absence of EF-G, which originate from residual direct excitation of the mant group at the excitation wavelength used for FRET, were measured and subtracted. For further calculations, the values were normalized by assigning the highest value in the titration to 1 and the lowest to 0. The titration curve was evaluated by the equation $\Delta F = 0.5B_{max}/P(K_d + P + X) - \mathrm{sqrt}((K_d + P + X)^2 - 4PX)$, where B_{max} is the amplitude (a value close to 1), P is the total concentration of EF-G, X is total concentration of nucleotide, and K_d is the dissociation constant.

RESULTS AND DISCUSSION

Sequences of Initiation and Elongation Factors. Msm genes encoding initiation and elongation factors were identified by Blast search using the respective *E. coli* sequences. The gene assignment based on sequence alignments was confirmed by the primary annotation of *M. smegmatis* genes on the TIGR-CMR Web site (http://www.tigr.org, The Institute for Genomic Research, Comprehensive Microbial Resources). Individual translation factors were aligned with their bacterial, archeal, and eukaryotic counterparts, and the secondary structures were assigned based on the available NMR and crystal structures (Figures 1–3).

Msm IF1 has 98% sequence identity to *M. tuberculosis* and 65% identity to *Eco* and *T. thermophilus* factors. Given this high sequence conservation, the structure of *Msm* IF1 is likely to be similar to the β-barrel structure of *Eco* IF1 (*39*) (Figure 1). In eukaryotes, the core eIF1A comprising

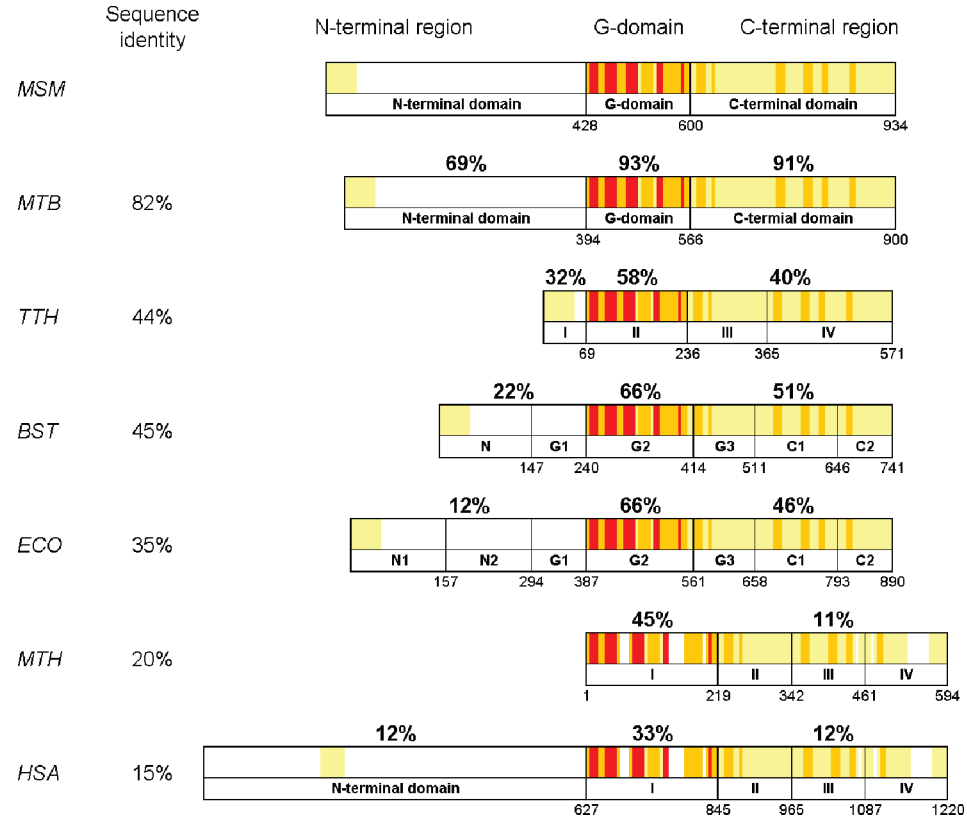

FIGURE 2: Sequence alignments of selected IF2/eIF5B homologues. Domain structure and overall sequence conservation among eukaryotic, archeal, and prokaryotic IF2 sequences in the N-terminal region, the GTP-binding domain (G-domain), and the C-terminal region of the proteins. The overall sequence identity is shown on the left as percentage compared to *M. smegmatis* IF2. IF2 sequences are from MSM, *Mycobacterium smegmatis* (GenBank accession number CP000480); MTB, *Mycobacterium tuberculosis* (CAB03670.1); TTH, *Thermus thermophilus* (AAS80695.1); BST, *Bacillus stearothermophilus* (CAA27987); ECO, *Escherichia coli* (AAC76202.1); MTH, *Methanobacter thermautotropicus* (AAB84765); and HSA, *Homo sapiens* (NP_056988). The secondary structure elements indicated at the top are taken from *E. coli* IF2 (PDB 1zo1 (*48*)) and at the bottom from *M. thermoautotropicus* eEF5B (PDB 1g7t (*46*)). Symbols and colors are as in Figure 1.

five β-sheets and an α-helix represents the structural and functional homologue of bacterial IF1. The N- and C-terminal extensions of eIF1A are not found in bacterial IF1 and may play a specialized role in eukaryotic translation initiation (*40–42*).

The domain structure of *Msm* IF2 is very similar to that of the *Eco* factor (Figure 2), which consists of the N- and C-terminal regions and the middle GTP binding domain. The N-terminal region in bacteria is variable in length and is not conserved except for the first 50 amino acids, which form a compact N1 domain (*43*), the function of which is not known. N2 domain of *Eco* IF2 has high binding affinity to the 30S subunit (*44*); otherwise its function is not known. In eukaryotes the N-terminal region is even more variable and was found to be not essential, as N-terminally truncated ΔeIF5B$_{587-1220}$ was fully active (*45*). Archeal aIF5B completely lacks the N-terminal portion (*46*). The N-terminal domain is disordered in the cryo-EM structures of ribosomes with IF2 (*47, 48*) and is connected to the G-domain by a flexible linker. The G-domain of bacterial, archeal, and eukaryotic IF2/eIF5B is highly conserved, particularly at the functionally important regions, i.e., the P loop as well as switch 1 and switch 2 regions, and is similar to the G-domains of other translation factors, such as EF-Tu and EF-G. The C-terminal part of IF2 is responsible for recognition of fMet-tRNA^{fMet} and positioning of tRNA with respect to the ribosome (*1, 49*); this part is well to moderately conserved and is present in IF2 sequences from all kingdoms.

Bacterial IF3 consists of two domains, the N- and C-terminal, connected by a flexible linker (*50*). *Msm* IF3 is similar in length and sequence to other bacterial IF3s and is 45% and 51% identical to *Eco* and *B. stearothermophilus* IF3, respectively (Figure 3). Although there is little sequence conservation between bacterial IF3 and eukaryotic eIF1 (<15% identity), the factors have similar functions in initiation codon selection, bind to the same region on the ribosome, and can even function in heterologous initiation assays (*51–53*). One major difference in IF3 sequences from different organisms is the length of the N- and C-terminal extensions, and the N-terminal extension is particularly long in *Msm* IF3. Given the sequence similarity, the N-terminal domain of *Msm* IF3 is likely to form a domain similar to that of *B. stearothermophilus* IF3 (*54*). However, in other organisms, e.g., *T. thermophilus* IF3 or in eukaryotic eIF1, a large part of the N-terminal domain is not present, and the region is unstructured (*55, 56*). The C-terminal domain has a two-layer sandwich fold in pro- and eukaryotes (*50, 54–56*) and is in bacteria capable of performing all of the functions of intact IF3 (1). The function of the long C-terminal extension characteristic for *Msm* IF3 is not known.

The sequences of elongation factors, EF-Tu and EF-G, are highly conserved within all bacteria. Sequence identity of *Msm* EF-Tu compared to *M. tuberculosis*, *T. thermophilus*, and *Eco* EF-Tu is 95%, 71%, and 75%, respectively, and that of EF-G is 87%, 60%, and 59%, respectively; taking

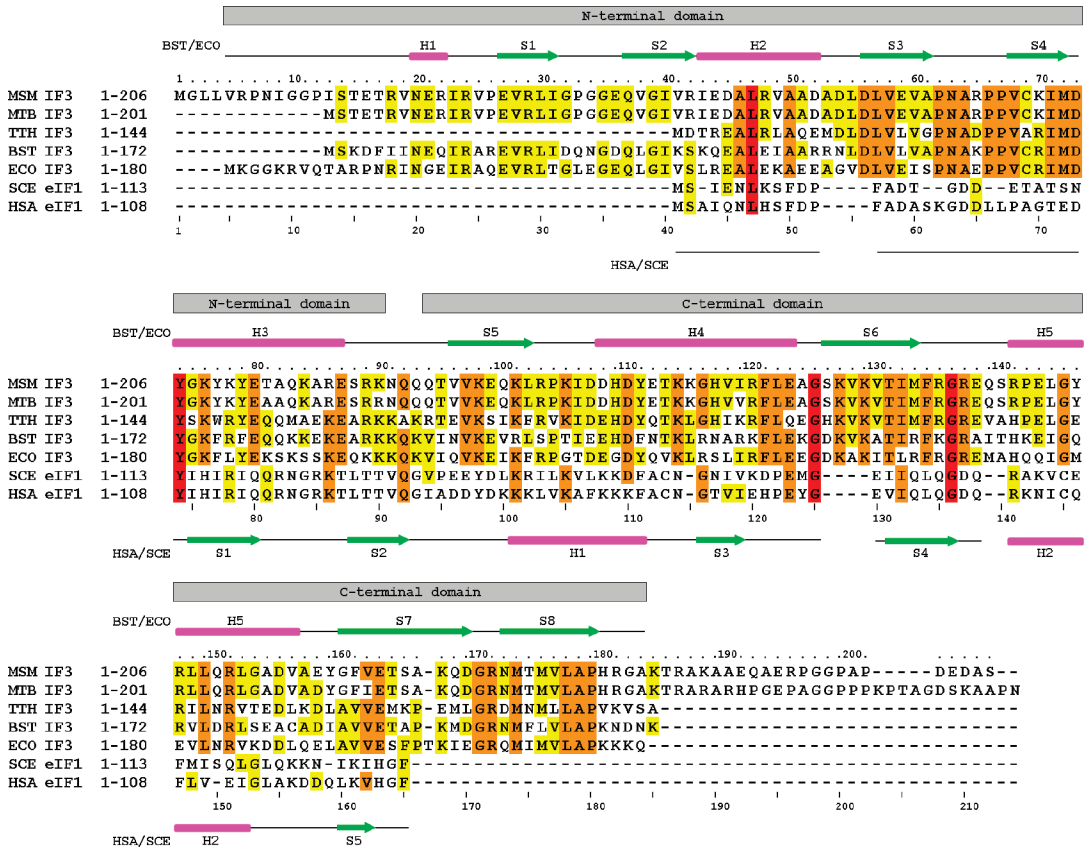

FIGURE 3: Multiple sequence alignments of bacterial IF3 and eukaryotic eIF1. Sequences of IF3 are from MSM, *Mycobacterium smegmatis* (GenBank accession number CP000480); MTB, *Mycobacterium tuberculosis* (CAB06651.1); TTH, *Thermus thermophilus* (AAS80531.1); BST, *Bacillus stearothermophilus* (CAA34312); ECO, *Escherichia coli* (AAC74788.1); eIF1 from SCE, *Saccharomyces cerevisiae* (EDN62581); and HSA, *Homo sapiens* (P41567). The secondary structure elements indicated at the top are from *E. coli* and *B. stearothermophilus* IF3 (PBP 2ife (*50*); 1tig and 1tif (*54*)) and at the bottom from *H. sapiens* and *S. cerevisiae* IF1(PDB 2if1 (*56*) and 2ogh (*55*)). Symbols and colors are as in Figure 1.

into account neutral amino acid substitutions the structures of the factors are expected to be very similar. Identified genes of initiation and elongation factors were PCR-amplified from *Msm* genomic DNA and cloned into expression vectors as described in Materials and Methods. Recombinant proteins were overexpressed in *Eco* and purified using an N-terminal $(His)_6$ tag.

Functions of Initiation Factors. The functions of initiation factors, as identified in the *Eco* system, include (i) facilitating the dissociation of 70S ribosomes into the 30S and 50S subunits, (ii) delivery of fMet-tRNA^{fMet} to the P site, and (iii) controlling the fidelity of initiation depending on the start codon and the properties of the translation initiation region (TIR). Each initiation factor has its specific role in initiation; in addition, the factors affect the activity of one another. To test the activity of *Msm* IFs, we first measured the binding of f[^{3}H]Met-tRNA^{fMet} to *Msm* 70S ribosomes in the presence of mRNA and different combinations of IFs (Figure 4a), which is the most sensitive assay for the activity of all three IFs at once. In the presence of all initiation factors, 70% of ribosomes were loaded with fMet-tRNA^{fMet}. The 70S IC formation is strongly IF2-dependent which indicates that IF2 is the principle factor responsible for fMet-tRNA^{fMet} delivery. Omission of either IF1 or IF3, which is expected to affect subunits' dissociation, decreased the extent of initiation, similarly to the effects observed in the *Eco* system. Titration with IFs suggested that when both subunits are present, catalytic amounts of IF2 were sufficient for the 70S IC formation (Figure 4b), which suggests that IF2 makes efficient turnover on 70S ribosomes. In contrast, a molar excess of IF1 and IF3 was required to reach maximum initiation efficiency. The activity of *Eco* IF2 on the 30S subunit is modulated by IF1 which accelerates the 30S initiation complex formation (*57*). The stimulation of *Msm* 30S initiation complex formation by *Msm* IF1 was tested at initial velocity conditions (Figure 4c). At limiting IF2 concentrations, about 2-fold stimulation by IF1 of fMet-tRNA^{fMet} binding to the 30S subunit was observed. Thus, also this aspect of initiation complex formation is similar in the *Msm* and *Eco* systems.

While the main function of IF2 is to deliver fMet-tRNA^{fMet} to the 30S subunit, IF1 and IF3 have pleiotropic effects on initiation. Functions of IF3 reported for the *Eco* system include (i) inhibition of subunit association, (ii) control of initiation fidelity, (iii) acceleration of 30S IC formation, and (iv) adjustments of mRNA position in the 70S IC (1). IF1 was found to (i) increase the binding of IF2 and fMet-tRNA^{fMet} to the 30S subunit, (ii) support the subunit antiassociation function of IF3 and increase the rate of IF3-independent dissociation of 70S ribosomes, and (iii) mediate IF3 function in control of initiation fidelity (1). In the following, we examine to which extent the same functions are carried out by *Msm* IF1 and IF3.

To test the activity of *Msm* IF3 in inhibition of subunit association, we purified *Msm* 30S and 50S subunits. The association of the ribosomal subunits into 70S ribosomes was

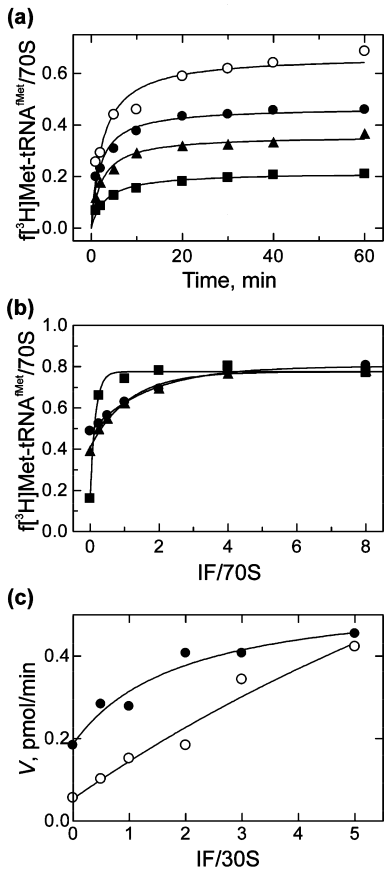

FIGURE 4: Activity of *M. smegmatis* initiation factors. (a) Initiation in the presence of all initiation factors (○; 1 μM each) or in the absence of IF1 (●), IF2 (■), or IF3 (▲). (b) Initiation with different amounts of IF1 (●), IF2 (■), or IF3 (▲) in the presence of the two other initiation factors (1 μM each). (c) Stimulation of IF2 activity by IF1. Initial velocity of binding of f[^{3}H]Met-tRNA^{fMet} was measured at increasing concentration of IF2 alone (○) and in the presence of IF2 (0.5 μM) and increasing concentration of IF1 (●).

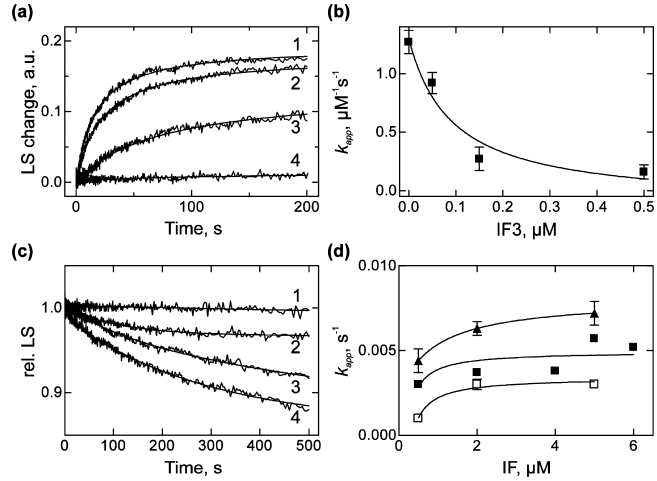

FIGURE 5: Effect of initiation factors on association and dissociation of ribosomal subunits. (a) Association of 30S and 50S subunits (0.05 μM each) in the absence of IF3 (1) and in the presence of increasing IF3 concentrations (0.05 μM, trace 2; 0.15 μM, trace 3; or 0.5 μM, trace 4). LS, light scattering; a.u., arbitrary units. (b) Concentration dependence of the apparent association rate constant (k_{app}) on IF3. (c) Dissociation of 70S ribosomes (0.05 μM) in buffer A in the absence of the factors (trace 1) and in the presence of IF1 alone (trace 2), IF3 alone (trace 3), or IF1 and IF3 together (trace 4); initiation factors were added at 2 μM concentration each. (d) Concentration dependence of the k_{app} values of 70S (0.05 μM) dissociation into subunits in the presence of IF1 alone (▲), IF3 alone (□), or IF1 and IF3 together (●). In the latter case, concentrations of IF3 were as indicated and of IF1 twice as high.

monitored by changes in light scattering (*37*). In the absence of IFs, the ribosomal subunits quickly assembled into 70S ribosomes (Figure 5a). In the absence of IF3, the rate of subunit association $k_{assoc} = 1.3 \pm 0.1$ μM^{-1} s^{-1} is well within the range of rate constants reported for the association of the *Eco* ribosome subunits, between $k_{assoc} = 1.2$ μM^{-1} s^{-1} (*58*) to 6 μM^{-1} s^{-1} (*34*). IF3 prevented subunit association in a dose-dependent manner. In the presence of excess IF3, subunit association is abolished (Figure 5a,b), which is also observed in the *Eco* system (*34, 37, 58*). Notably, such a strong inhibition is observed only in the absence of initiator tRNA; with true 30S IC, IF3 decreases the rate of 50S subunit joining only by a factor of 9 (*59*). The concentration of IF3 at which the rate and the end point of subunit association were reduced by a factor of 2 is 0.07 μM (Figure 5b) and 0.1 μM (Figure 5a), respectively, which is close to the concentration of the 50S subunit in the reaction (0.05 μM). This suggests that IF3 and 50S subunits have similar affinities to 30S subunits, also quite consistent with the data obtained for *Eco* ribosomes and IF3 (*37*).

Spontaneous dissociation of 70S ribosomes is slow and reversible. By inhibiting subunit association (decreasing k_{assoc}; see above), IF3 increases the pool of free subunits and appears to facilitate 70S dissociation. Slow dissociation of *Msm* 70S ribosomes was observed in the presence of *Msm* IF3 (Figure 5c). The apparent rate constant of dissociation, $k_{dissoc} = 0.003 \pm 0.001$ s^{-1}, was practically independent of IF3 concentration (Figure 5d), which is expected at conditions of >5-fold factor excess over the presumed K_d value (see above). *Eco* IF1 has been reported to have a small but consistent effect on 70S dissociation by increasing the k_{dissoc} about 3-fold (*37*). Similarly, *Msm* IF1 enhances ribosome dissociation about 2-fold (Figure 5d). In the presence of IF1 alone the end point of 70S dissociation is significantly less than with IF3 or IF1 and IF3 together, suggesting that IF1 promotes dissociation of only a small part of the ribosomes. The portion of ribosomes which dissociate in the presence of IF1 increases with the factor concentration but does not reach the end point even in the presence of 5 μM IF1 (data not shown). Addition of *Msm* IF1 and IF3 together resulted in a larger portion of ribosomes dissociated into subunits and an intermediate $k_{dissoc} = 0.005 \pm 0.001$ s^{-1} value. Given the similarity of the k_{dissoc} values obtained with IF1 and IF3 alone or in the presence of both factors, the main effect on 70S dissociation appears to be the inhibition of subunit joining by IF3; IF1 has a very small stimulating effect.

One important IF3 function is the selection of initiator tRNA and the start codon (1). To test whether the *Msm* factor fulfills this function, a set of mRNAs was used with canonical AUG or noncanonical AUU start codons (Table 1), and initiation was measured by binding of fMet-tRNA^{fMet} to the ribosome (Figure 6). Similarly to the *Eco* system, selection of initiator tRNA in *Msm* is highly dependent on both the presence of a cognate start codon and the concentration of IF3. Neither the rare AUU start codon nor poly(U) form initiation complexes efficiently when IF3 is present. At very low concentrations of IF3 the selection of AUG as start codon

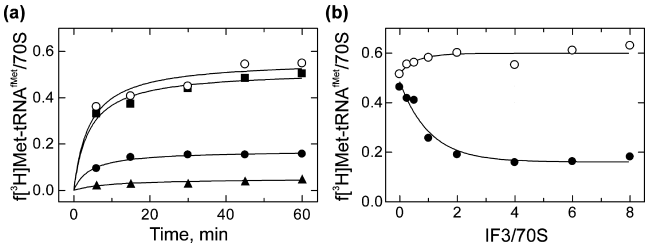

FIGURE 6: Effect of IF3 on fidelity of initiation. (a) 70S ribosomes (0.5 μM) and initiation factors (1 μM) were incubated with f[^{3}H]Met-tRNA^{fMet} (1 μM) and the following mRNAs (1.5 μM): AUG-(UUU)$_{12}$ (○), AUU-(UUU)$_{12}$ (●), MFTI-mRNA (■), and poly(U) (▲). (b) IF3 concentration dependence of initiation on AUG-(UUU)$_{12}$ (○) or AUU-(UUU)$_{12}$ (●). Reactions were analyzed after 30 min of incubation at 37 °C.

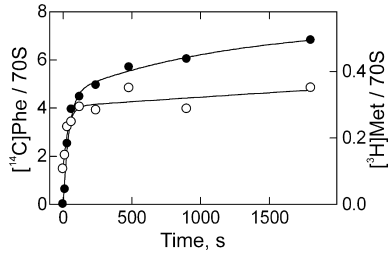

FIGURE 7: Translation of a AUG-(UUU)$_{12}$ mRNA by *M. smegmatis* ribosomes. Peptide length was followed by the number of [^{14}C]Phe incorporated per ribosome (●), the number of chains by [^{3}H]Met in peptides per ribosome (○).

is abolished, and initiation complexes are also formed on rare start codons.

Elongation Factors. Elongation phase of protein synthesis is promoted by two factors, EF-Tu and EF-G. To test whether the isolated *Msm* factors and ribosomes can synthesize full-length peptides, we translated an mRNA (AUG-(UUU)$_{12}$) coding for an fMet-(Phe)$_{12}$ peptide. 70S initiation complexes were formed with f[^{3}H]Met-tRNA^{fMet}, and translation was initiated by addition of a large excess of EF-Tu·GTP·[^{14}C]Phe-tRNA^{Phe} and EF-G (Figure 7). Within minutes the reaction was completed on 30% ribosomes, as indicated by the amount of f[^{3}H]Met in peptides. The mRNA was translated to the end, resulting in a Phe/fMet ratio of about 12. The rate of translation of each codon was 0.3 s^{-1} estimated from the overall rate of reaction and the chain length. In addition to the rapid and specific synthesis, a much slower (0.005 s^{-1} aa^{-1}) formation of [^{14}C]Phe chains was observed which did not contain [^{3}H]Met. This can be explained by a small portion of ribosomes which did not bind fMet-tRNA^{fMet} and after addition of Phe-tRNA^{Phe} started poly(Phe) synthesis on one of the internal UUU codons.

EF-Tu and EF-G are GTP/GDP binding proteins. *Eco* EF-Tu binds GDP very tightly, and the spontaneous dissociation of the EF-Tu·GDP complex is very slow (*60, 61*). However, such slow GDP dissociation from *Eco* EF-Tu may be unique among translational GTPases, because similar factors, notably the yeast homologue of EF-Tu, eEF1α, release the nucleotide much faster (*62*). To measure the rate of spontaneous nucleotide dissociation from *Msm* EF-Tu, we used mant-labeled nucleotides and monitored the dissociation of EF-Tu-bound mant-GDP upon addition of an excess of unlabeled GDP (Figure 8a). Addition of the mant group does not appreciably affect the properties of nucleotides with respect to their affinity to *Eco* EF-Tu or EF-G (*61, 63*). At high excess of unlabeled GDP, rebinding of mant-GDP is

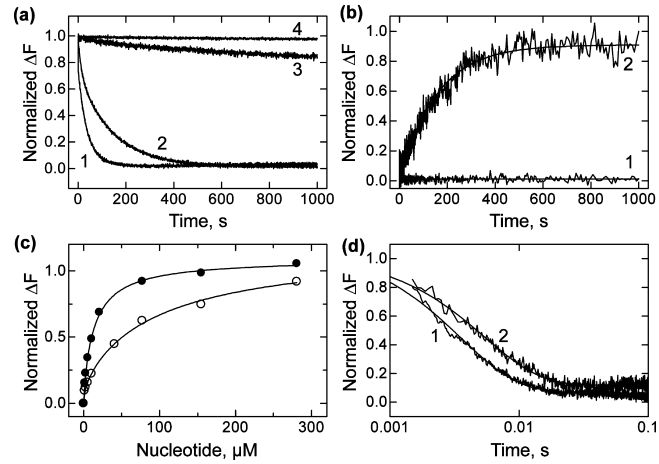

FIGURE 8: Nucleotide exchange in EF-Tu and EF-G. (a) Dissociation of mant-GDP from *Msm* EF-Tu upon addition of excess nonmodified GDP at 37 °C (1) or 20 °C (2) or upon dilution with the same buffer at 37 °C (3) or 20 °C (4). Normalized ΔF, FRET change rescaled between 0 (the lowest value) and 1 (the highest value). (b) Dissociation of EF-Tu·GTP upon dilution (1) or addition of excess mant-GTP at 20 °C (2). (c) Binding of *Msm* EF-G (2 μM) to mant-GTP (○) and mant-GDP (●). The lines show one-site binding fits (*63*). (d) Dissociation of mant-GDP (trace 1) and mant-GTP (trace 2) from *Msm* EF-G.

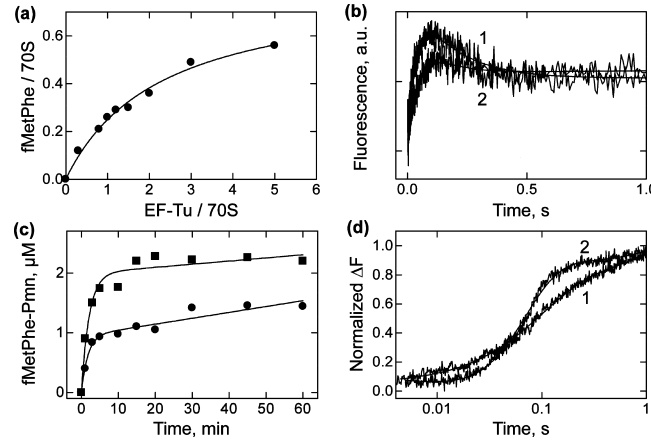

FIGURE 9: A-site binding and translocation. (a) Dependence of [^{14}C]Phe-tRNA^{Phe} binding on EF-Tu addition. Formation of fMetPhe dipeptide was measured. (b) Rapid kinetics of EF-Tu·GTP·[^{14}C]Phe-tRNA^{Phe}(Prf) (0.1 μM) binding to the 70S initiation complex (0.3 μM) with *Eco* (trace 1) and *Msm* (trace 2) components. (c) Multiple-turnover translocation. Time courses of translocation measured by Pmn reaction on *Msm* (●) and *Eco* (■) pretranslocation complexes with homologous EF-G. (d) Single-round translocation of mRNA(Flu) from the pre- to posttranslocation position with *Msm* (trace 1) or *Eco* (trace 2) components.

negligible, and the rate of dissociation corresponds to the k_{off} of the EF-Tu·GDP complex. The dissociation of *Msm* EF-Tu·mant-GDP complex was very slow, about 0.007 s^{-1} at 20 °C or 0.27 s^{-1} at 37 °C. The former value is close to that measured for the *Eco* EF-Tu·GDP complex, 0.002 s^{-1} at 20 °C (*61*). A very similar dissociation rate was found for *Msm* EF-Tu·GTP complex, 0.006 s^{-1} at 20 °C (Figure 8b). The latter reaction was followed using unlabeled EF-Tu·GTP upon addition of excess mant-GTP. Because binding of mant-GTP is limited by the dissociation rate of nonlabeled GTP, the observed rate reflects the k_{off} of the EF-Tu·GTP complex. This value was somewhat lower than that measured for GTP dissociation from *Eco* EF-Tu, 0.03 s^{-1} at 20 °C (*61*). The data suggest that *Msm* EF-Tu is active in

nucleotide binding and exchange, that the rates of nucleotide release are comparable to those reported for the *Eco* factor, and that, similarly to *Eco*, *Msm* EF-Tu requires a nucleotide exchange factor, EF-Ts, to release GDP rapidly enough to support protein synthesis in the cell.

In contrast to EF-Tu which has high affinity for GTP and GDP in the 0.1−0.01 μM range (*60, 61*), EF-G binds nucleotides weakly, with a K_d of 5−50 μM (*63*). To measure the affinity of *Msm* EF-G to GTP and GDP and the rates of nucleotide exchange, EF-G was first titrated with mant-GTP and mant-GDP (Figure 8c). The K_d values obtained from the titrations were 50 ± 9 μM (mant-GTP) and 12 ± 2 μM (mant-GDP). These values are within the range of K_d values reported earlier on the affinity of GTP and GDP binding to EF-G from *E. coli*, *T. thermophilus*, or *Thermotoga maritima*, although the exact K_d values vary within a factor of 10 between the organisms (*63–65*). The dissociation rate constants of GDP and GTP from EF-G were measured after mixing of EF-G·mant-GTP or EF-G·mant-GDP complexes with a large excess of unlabeled nucleotide (Figure 8d). In the presence of excess unlabeled nucleotide, rebinding of mant nucleotide to EF-G is abolished, and the observed rate reflects the dissociation rate constant, k_{off}. The dissociation of both mant-GDP and mant-GTP from *Msm* EF-G was very fast, 300 and 150 s^{-1}, respectively. The value for mant-GDP dissociation is very similar to that measured with *Eco* EF-G (*63*). However, the rate of mant-GTP release from *Msm* EF-G was much faster than from *E. coli* EF-G (7 s^{-1}) (*63*), which in part explains the difference in the K_d values of the *Msm* and *Eco* EF-G·mant-GTP complexes, 50 and 7 μM, respectively. The high rates of GDP dissociation indicate that nucleotide exchange occurs spontaneously and EF-G does not require a nucleotide exchange factor. From the equilibrium dissociation constant and the rate of nucleotide dissociation, the values of the association constants for mant-GDP and mant-GTP are 2.5×10^7 and 3×10^6 M^{-1} s^{-1}, respectively. At cellular concentrations of GTP in the millimolar range, the binding of nucleotide to EF-G is expected to be essentially instantaneous. Given that the affinity constants for GTP and GDP are similar, and GTP is present in a large excess over GDP, the factor will be rapidly loaded with GTP and will be found in the cell in the GTP form preferentially.

EF-Tu forms a ternary complex with Phe-tRNA^{Phe} and GTP, which binds to the A site of the translating ribosome. To test the ability of *Msm* EF-Tu to deliver aa-tRNA to the A site, 70S initiation complexes with fMet-tRNA^{fMet} in the P site were added with a slight excess of Phe-tRNA^{Phe} and increasing amount of EF-Tu·GTP (Figure 9a). As soon as Phe-tRNA^{Phe} is bound to the A site, peptidyl transfer takes place yielding a dipeptide fMetPhe (*32*), the formation of which was monitored. As expected, EF-Tu stimulated Phe-tRNA^{Phe} binding to the A site, suggesting that *Msm* EF-Tu was active in binding of both Phe-tRNA^{Phe} and the ribosome. To test whether the details of decoding are similar in the *Eco* and *Msm* systems, we used a rapid kinetics approach utilizing fluorescence changes of Phe-tRNA^{Phe}(Prf) at different steps of decoding (*66*). Binding of the ternary complex to *Msm* ribosomes led to a series of fluorescence changes very similar to those observed in the *Eco* system (Figure 9b). The extensive work on step assignment on *Eco* ribosomes suggested that the first step (k_{app1}) reflects the binding and codon recognition steps (*38, 67*). The amplitude of the fluorescence change and the rate of this step are comparable in *Eco* and *Msm* systems, 23 ± 2 and 13 ± 3 s^{-1}. This indicates that EF-Tu-dependent aa-tRNA delivery to the A site is not faster to the ribosomes from *Msm* compared to *Eco*, despite the extended factor-binding stalk with six copies of L12. The second step (fluorescence decrease, k_{app2}) is a complex step resulting from at least two rearrangements: a decomposition of the GTPase-activated state of EF-Tu and a concomitant accommodation of aa-RNA in the A site. The two steps have a similar rate on *Eco* ribosomes and thus cannot be distinguished kinetically (*38*). The GTPase intermediate is the high-fluorescence state; it can be blocked by kirromycin in a conformation where the structure of tRNA is distorted (*68, 69*), hence the fluorescence change of the reporter group at the elbow region of tRNA (*38*). The k_{app2} values are also similar for *Eco* and *Msm*, 7 ± 1 and 11 ± 2 s^{-1}, respectively. The data suggest that the detailed kinetics of decoding is quite similar in the two model systems, which implies a high degree of evolutionary conservation of translation mechanisms among different bacteria, despite the different composition of the L12 stalk.

EF-G catalyzes translocation of peptidyl-tRNA from the A site to the P site. The activity of *Msm* EF-G in translocation was tested in a multiple-turnover assay with catalytic amounts of EF-G (0.5 nM) and excess of pretranslocation complexes with f[^{3}H]MetPhe-tRNA^{Phe} in the A site (2 μM). The high concentration of the pretranslocation complex was chosen in order to determine the rates of reaction at substrate saturation where the measured initial velocity is proportional to k_{cat} ($V_{max} = k_{cat}$[EF-G]) (Figure 9c). fMetPhe-tRNA^{Phe} which was translocated to the P site was detected by puromycin (Pmn) reaction; the Pmn reaction itself is very rapid (about 10 s^{-1} at the conditions used (*32*)) compared to multiple-turnover translocation. During the reaction, translocation occurred on the majority of ribosomes, i.e., on 100% of *Eco* and >60% of *Msm* pretranslocation complexes. Comparing the concentration of the resulting posttranslocation complexes with the EF-G concentration indicates that *Eco* and *Msm* EF-G performed 4000 and 2400 turnovers, respectively. The velocity of multiple-turnover translocation was calculated from the initial parts of time courses (Figure 9c) which yield V_{max} (μM/min) at conditions of substrate saturation. The calculated k_{cat} values were 15 and 9 s^{-1} for *Eco* and *Msm* factors, respectively. These values provide the lower limit to the rate constant of tRNA movement through the ribosome, because additional steps, such as EF-G dissociation from the ribosome and nucleotide exchange, are likely to contribute to the k_{cat} value.

To assess the rate of tRNA−mRNA movement directly, we used a rapid kinetics assay following the movement of mRNA(Flu) (*70*). Pretranslocation complexes contained mRNA(Flu) and fMetPhe-tRNA^{Phe} bound to the A site, and translocation was initiated by addition of saturating amount of EF-G (Figure 9d). The rate constants of mRNA-tRNA movement through the ribosome were 22 and 11 s^{-1} with *Eco* and *Msm* EF-G, respectively. This indicates that *Msm* EF-G promotes translocation at rates comparable to the expected rates of protein synthesis in the cell, 10−20 s^{-1}. The similarity of detailed kinetics suggests a high degree of evolutionary conservation of ribosome and factor functions during initiation and elongation of translation.

In conclusion, a high degree of conservation in the mechanisms of translation between *E. coli* and *M. smegmatis* has been observed in several biochemical assays that tested individual steps in translation initiation and elongation, establishing the *M. smegmatis* translation system reconstituted from purified components as a well-defined active experimental assay. Despite differences in protein and nucleotide sequences of factors and rRNA, different sensitivity to mutations at the active sites, and different composition of the L12 stalk, the translational machinery works with very similar efficiencies in *M. smegmatis* and *E. coli*. While the structure of the *M. smegmatis* ribosome is much less sensitive to mutational alterations compared to that from *E. coli*, the similarity of detailed kinetics indicates that translation factors have coevolved with the ribosome in such a way as to maintain an optimal rate of translation reactions.

The availability of a purified reconstituted translation system from *M. smegmatis* allows for systematic biochemical and genetic studies in a model organism different from *E. coli*. *M. smegmatis* has a number of advantages over *E. coli*, not the least its accessibility to genetic manipulations, particularly in introducing mutations into rRNA (*29, 31*). *M. smegmatis* is tolerant to a number of mutations that render lethal phenotypes in *E. coli* (*8, 32*), which allows for the preparation of homogeneous mutant ribosomes without the use of tag systems. We anticipate employing the reconstituted *Msm* translation system to further understand the molecular basis of translation and to develop systems for testing the activity of antimicrobial compounds (*14, 71–73*).

ACKNOWLEDGMENT

The authors thank Peter Pfister for help in the initial phase of the project, Akshay Subramanian for valuable contributions to factor cloning, and Carmen Schillings, Astrid Böhm, Simone Möbitz, Petra Striebeck, and Tanja Janušić for expert technical assistance.

REFERENCES

1. Gualerzi, C. O., Brandi, L., Caserta, E., Garofalo, C., Lammi, M., La Teana, A., Petrelli, D., Spurio, R., Tomsic, J., and Pon, C. L. (2001) Initiation factors in the early events of mRNA translation in bacteria. *Cold Spring Harbor Symp. Quant. Biol. 66*, 363–376.
2. Karimi, R., Pavlov, M. Y., Buckingham, R. H., and Ehrenberg, M. (1999) Novel roles for classical factors at the interface between translation termination and initiation. *Mol. Cell 3*, 601–609.
3. Peske, F., Rodnina, M. V., and Wintermeyer, W. (2005) Sequence of steps in ribosome recycling as defined by kinetic analysis. *Mol. Cell 18*, 403–412.
4. Hirashima, A., and Kaji, A. (1970) Factor dependent breakdown of polysomes. *Biochem. Biophys. Res. Commun. 41*, 877–883.
5. Cannone, J. J., Subramanian, S., Schnare, M. N., Collett, J. R., D'Souza, L. M., Du, Y., Feng, B., Lin, N., Madabusi, L. V., Muller, K. M., Pande, N., Shang, Z., Yu, N., and Gutell, R. R. (2002) The comparative RNA web (CRW) site: an online database of comparative sequence and structure information for ribosomal, intron, and other RNAs. *BMC Bioinformatics 3*, 15.
6. Laursen, B. S., Sorensen, H. P., Mortensen, K. K., and Sperling-Petersen, H. U. (2005) Initiation of protein synthesis in bacteria. *Microbiol. Mol. Biol. Rev. 69*, 101–123.
7. Caetano-Anolles, G. (2002) Tracing the evolution of RNA structure in ribosomes. *Nucleic Acids Res. 30*, 2575–2587.
8. Sander, P., Belova, L., Kidan, Y. G., Pfister, P., Mankin, A. S., and Bottger, E. C. (2002) Ribosomal and non-ribosomal resistance to oxazolidinones: species-specific idiosyncrasy of ribosomal alterations. *Mol. Microbiol. 46*, 1295–1304.
9. Pfister, P., Risch, M., Brodersen, D. E., and Böttger, E. C. (2003) Role of 16S rRNA helix 44 in ribosomal resistance to hygromycin B. *Antimicrob. Agents Chemother. 47*, 1496–1502.
10. Xiong, L., Polacek, N., Sander, P., Bottger, E. C., and Mankin, A. (2001) pKa of adenine 2451 in the ribosomal peptidyl transferase center remains elusive. *RNA 7*, 1365–1369.
11. Beringer, M., Adio, S., Wintermeyer, W., and Rodnina, M. (2003) The G2447A mutation does not affect ionization of a ribosomal group taking part in peptide bond formation. *RNA 9*, 919–922.
12. Recht, M. I., Douthwaite, S., Dahlquist, K. D., and Puglisi, J. D. (1999) Effect of mutations in the A site of 16 S rRNA on aminoglycoside antibiotic-ribosome interaction. *J. Mol. Biol. 286*, 33–43.
13. Hobbie, S. N., Pfister, P., Bruell, C., Sander, P., Francois, B., Westhof, E., and Böttger, E. C. (2006) Binding of neomycin-class aminoglycoside antibiotics to mutant ribosomes with alterations in the A-site of 16S rRNA. *Antimicrob. Agents Chemother. 50*, 1489–1496.
14. Hobbie, S. N., Pfister, P., Brull, C., Westhof, E., and Böttger, E. C. (2005) Analysis of the contribution of individual substituents in 4,6-aminoglycoside-ribosome interaction. *Antimicrob. Agents Chemother. 49*, 5112–5118.
15. Pfister, P., Hobbie, S., Vicens, Q., Böttger, E. C., and Westhof, E. (2003) The molecular basis for A-Site mutations conferring aminoglycoside resistance: relationship between ribosomal susceptibility and X-ray crystal structures. *ChemBioChem. 4*, 1078–1088.
16. Maki, Y., Hashimoto, T., Zhou, M., Naganuma, T., Ohta, J., Nomura, T., Robinson, C. V., and Uchiumi, T. (2007) Three binding sites for stalk protein dimers are generally present in ribosomes from archaeal organism. *J. Biol. Chem. 282*, 32827–32833.
17. Diaconu, M., Kothe, U., Schlunzen, F., Fischer, N., Harms, J. M., Tonevitsky, A. G., Stark, H., Rodnina, M. V., and Wahl, M. C. (2005) Structural basis for the function of the ribosomal L7/12 stalk in factor binding and GTPase activation. *Cell 121*, 991–1004.
18. Ilag, L. L., Videler, H., McKay, A. R., Sobott, F., Fucini, P., Nierhaus, K. H., and Robinson, C. V. (2005) Heptameric $(L12)_6$/L10 rather than canonical pentameric complexes are found by tandem MS of intact ribosomes from thermophilic bacteria. *Proc. Natl. Acad. Sci. U.S.A. 102*, 8192–8197.
19. Wimberly, B. T., Brodersen, D. E., Clemons, W. M., Jr., Morgan-Warren, R. J., Carter, A. P., Vonrhein, C., Hartsch, T., and Ramakrishnan, V. (2000) Structure of the 30S ribosomal subunit. *Nature 407*, 327–339.
20. Yusupov, M. M., Yusupova, G. Z., Baucom, A., Lieberman, K., Earnest, T. N., Cate, J. H., and Noller, H. F. (2001) Crystal structure of the ribosome at 5.5 Å resolution. *Science 292*, 883–896.
21. Ban, N., Nissen, P., Hansen, J., Moore, P. B., and Steitz, T. A. (2000) The complete atomic structure of the large ribosomal subunit at 2.4 Å resolution. *Science 289*, 905–920.
22. Schuwirth, B. S., Borovinskaya, M. A., Hau, C. W., Zhang, W., Vila-Sanjurjo, A., Holton, J. M., and Cate, J. H. (2005) Structures of the bacterial ribosome at 3.5 A resolution. *Science 310*, 827–834.
23. Selmer, M., Dunham, C. M., Murphy, F. V. t., Weixlbaumer, A., Petry, S., Kelley, A. C., Weir, J. R., and Ramakrishnan, V. (2006) Structure of the 70S ribosome complexed with mRNA and tRNA. *Science 313*, 1935–1942.
24. Harms, J., Schluenzen, F., Zarivach, R., Bashan, A., Gat, S., Agmon, I., Bartels, H., Franceschi, F., and Yonath, A. (2001) High resolution structure of the large ribosomal subunit from a mesophilic eubacterium. *Cell 107*, 679–688.
25. Thompson, J., and Dahlberg, A. E. (2004) Testing the conservation of the translational machinery over evolution in diverse environments: assaying *Thermus thermophilus* ribosomes and initiation factors in a coupled transcription-translation system from *Escherichia coli*. *Nucleic Acids Res. 32*, 5954–5961.
26. Wolfrum, A., Brock, S., Mac, T., and Grillenbeck, N. (2003) Expression in *E. coli* and purification of *Thermus thermophilus* translation initiation factors IF1 and IF3. *Protein Expression Purif. 29*, 15–23.
27. Day, J. M., and Janssen, G. R. (2004) Isolation and characterization of ribosomes and translation initiation factors from the gram-positive soil bacterium *Streptomyces lividans*. *J. Bacteriol. 186*, 6864–6875.
28. Janata, J., and Mikulik, K. (1995) Translation initiation factors of a tetracycline-producing strain of *Streptomyces aureofaciens*. *Biochem. Biophys. Res. Commun. 208*, 569–575.

29. Hobbie, S. N., Bruell, C., Kalapala, S. K., Akshay, S., Schmidt, S., Pfister, P., and Böttger, E. C. (2006) A genetic model to investigate structural drug-target interactions at the ribosomal decoding site. *Biochimie 88*, 1033–1043.
30. Sander, P., Prammananan, T., and Bottger, E. C. (1996) Introducing mutations into a chromosomal rRNA gene using a genetically modified eubacterial host with a single rRNA operon. *Mol. Microbiol. 22*, 841–848.
31. Hobbie, S. N., Kalapala, S. K., Akshay, S., Bruell, C., Schmidt, S., Dabow, S., Vasella, A., Sander, P., and Bottger, E. C. (2007) Engineering the rRNA decoding site of eukaryotic cytosolic ribosomes in bacteria. *Nucleic Acids Res. 35*, 6086–6093.
32. Beringer, M., Bruell, C., Xiong, L., Pfister, P., Bieling, P., Katunin, V. I., Mankin, A. S., Böttger, E. C., and Rodnina, M. V. (2005) Essential mechanisms in the catalysis of peptide bond formation on the ribosome. *J. Biol. Chem. 280*, 36065–36072.
33. Hobbie, S. N., Bruell, C. M., Akshay, S., Kalapala, S. K., Shcherbakov, D., and Bottger, E. C. (2008) Mitochondrial deafness alleles confer misreading of the genetic code. *Proc. Natl. Acad. Sci. USA 105*, 3244–3249.
34. Milon, P., Konevega, A. L., Peske, F., Fabbretti, A., Gualerzi, C. O., and Rodnina, M. V. (2007) Transient kinetics, fluorescence, and FRET in studies of initiation of translation in bacteria. *Methods Enzymol. 430*, 1–30.
35. Rodnina, M. V., and Wintermeyer, W. (1995) GTP consumption of elongation factor Tu during translation of heteropolymeric mRNAs. *Proc. Natl. Acad. Sci. U.S.A. 92*, 1945–1999.
36. Rodnina, M. V., Savelsbergh, A., Matassova, N. B., Katunin, V. I., Semenkov, Y. P., and Wintermeyer, W. (1999) Thiostrepton inhibits the turnover but not the GTPase of elongation factor G on the ribosome. *Proc. Natl. Acad. Sci. U.S.A. 96*, 9586–9590.
37. Godefroy-Colburn, T., Wolfe, A. D., Dondon, J., and Grunberg-Manago, M. (1975) Light-scattering studies showing the effect of initiation factors on the reversible dissociation of *Escherichia coli* ribosomes. *J. Mol. Biol. 94*, 461–478.
38. Rodnina, M. V., Fricke, R., and Wintermeyer, W. (1994) Transient conformational states of aminoacyl-tRNA during ribosome binding catalyzed by elongation factor Tu. *Biochemistry 33*, 12267–12275.
39. Sette, M., van Tilborg, P., Spurio, R., Kaptein, R., Paci, M., Gualerzi, C. O., and Boelens, R. (1997) The structure of the translational initiation factor IF1 from *E. coli* contains an oligomer-binding motif. *EMBO J. 16*, 1436–1443.
40. Olsen, D. S., Savner, E. M., Mathew, A., Zhang, F., Krishnamoorthy, T., Phan, L., and Hinnebusch, A. G. (2003) Domains of eIF1A that mediate binding to eIF2, eIF3 and eIF5B and promote ternary complex recruitment *in vivo*. *EMBO J. 22*, 193–204.
41. Fekete, C. A., Mitchell, S. F., Cherkasova, V. A., Applefield, D., Algire, M. A., Maag, D., Saini, A. K., Lorsch, J. R., and Hinnebusch, A. G. (2007) N- and C-terminal residues of eIF1A have opposing effects on the fidelity of start codon selection. *EMBO J. 26*, 1602–1614.
42. Fekete, C. A., Applefield, D. J., Blakely, S. A., Shirokikh, N., Pestova, T., Lorsch, J. R., and Hinnebusch, A. G. (2005) The eIF1A C-terminal domain promotes initiation complex assembly, scanning and AUG selection *in vivo*. *EMBO J. 24*, 3588–3601.
43. Laursen, B. S., Mortensen, K. K., Sperling-Petersen, H. U., and Hoffman, D. W. (2003) A conserved structural motif at the N terminus of bacterial translation initiation factor IF2. *J. Biol. Chem. 278*, 16320–16328.
44. Caserta, E., Tomsic, J., Spurio, R., La Teana, A., Pon, C. L., and Gualerzi, C. O. (2006) Translation initiation factor IF2 interacts with the 30 S ribosomal subunit via two separate binding sites. *J. Mol. Biol. 362*, 787–799.
45. Pestova, T. V., Lomakin, I. B., Lee, J. H., Choi, S. K., Dever, T. E., and Hellen, C. U. (2000) The joining of ribosomal subunits in eukaryotes requires eIF5B. *Nature 403*, 332–325.
46. Roll-Mecak, A., Cao, C., Dever, T. E., and Burley, S. K. (2000) X-Ray structures of the universal translation initiation factor IF2/eIF5B: conformational changes on GDP and GTP binding. *Cell 103*, 781–792.
47. Myasnikov, A. G., Marzi, S., Simonetti, A., Giuliodori, A. M., Gualerzi, C. O., Yusupova, G., Yusupov, M., and Klaholz, B. P. (2005) Conformational transition of initiation factor 2 from the GTP- to GDP-bound state visualized on the ribosome. *Nat. Struct. Mol. Biol. 12*, 1145–1149.
48. Allen, G. S., Zavialov, A., Gursky, R., Ehrenberg, M., and Frank, J. (2005) The cryo-EM structure of a translation initiation complex from *Escherichia coli*. *Cell 121*, 703–712.
49. Allen, G. S., and Frank, J. (2007) Structural insights on the translation initiation complex: ghosts of a universal initiation complex. *Mol. Microbiol. 63*, 941–950.
50. Moreau, M., de Cock, E., Fortier, P. L., Garcia, C., Albaret, C., Blanquet, S., Lallemand, J. Y., and Dardel, F. (1997) Heteronuclear NMR studies of *E. coli* translation initiation factor IF3. Evidence that the inter-domain region is disordered in solution. *J. Mol. Biol. 266*, 15–22.
51. Lomakin, I. B., Kolupaeva, V. G., Marintchev, A., Wagner, G., and Pestova, T. V. (2003) Position of eukaryotic initiation factor eIF1 on the 40S ribosomal subunit determined by directed hydroxyl radical probing. *Genes Dev. 17*, 2786–2797.
52. Lomakin, I. B., Shirokikh, N. E., Yusupov, M. M., Hellen, C. U., and Pestova, T. V. (2006) The fidelity of translation initiation: reciprocal activities of eIF1, IF3 and YciH. *EMBO J. 25*, 196–210.
53. Pestova, T. V., and Kolupaeva, V. G. (2002) The roles of individual eukaryotic translation initiation factors in ribosomal scanning and initiation codon selection. *Genes Dev. 16*, 2906–2922.
54. Biou, V., Shu, F., and Ramakrishnan, V. (1995) X-ray crystallography shows that translational initiation factor IF3 consists of two compact alpha/beta domains linked by an α helix. *EMBO J. 14*, 4056–4064.
55. Reibarkh, M., Yamamoto, Y., Singh, C. R., del Rio, F., Fahmy, A., Lee, B., Luna, R. E., Ii, M., Wagner, G., and Asano, K. (2008) Eukaryotic initiation factor (eIF) 1 carries two distinct eIF5-binding faces important for multifactor assembly and AUG selection. *J. Biol. Chem. 283*, 1094–1103.
56. Fletcher, C. M., Pestova, T. V., Hellen, C. U., and Wagner, G. (1999) Structure and interactions of the translation initiation factor eIF1. *EMBO J. 18*, 2631–2637.
57. Stringer, E. A., Sarkar, P., and Maitra, U. (1977) Function of initiation factor 1 in the binding and release of initiation factor 2 from ribosomal initiation complexes in *Escherichia coli*. *J. Biol. Chem. 252*, 1739–1744.
58. Antoun, A., Pavlov, M. Y., Tenson, T., and Ehrenberg, M. (2004) Ribosome formation from subunits studied by stopped-flow and Rayleigh light scattering. *Biol. Proced. Online 6*, 35–54.
59. Antoun, A., Pavlov, M. Y., Lovmar, M., and Ehrenberg, M. (2006) How initiation factors tune the rate of initiation of protein synthesis in bacteria. *EMBO J. 25*, 2539–2550.
60. Wagner, A., Simon, I., Sprinzl, M., and Goody, R. S. (1995) Interaction of guanosine nucleotides and their analogs with elongation factor Tu from *Thermus thermophilus*. *Biochemistry 34*, 12535–12542.
61. Gromadski, K. B., Wieden, H. J., and Rodnina, M. V. (2002) Kinetic mechanism of elongation factor Ts-catalyzed nucleotide exchange in elongation factor Tu. *Biochemistry 41*, 162–169.
62. Gromadski, K. B., Schummer, T., Stromgaard, A., Knudsen, C. R., Kinzy, T. G., and Rodnina, M. V. (2007) Kinetics of the interactions between yeast elongation factors 1A and 1Balpha, guanine nucleotides, and aminoacyl-tRNA. *J. Biol. Chem. 282*, 35629–35637.
63. Wilden, B., Savelsbergh, A., Rodnina, M. V., and Wintermeyer, W. (2006) Role and timing of GTP binding and hydrolysis during EF-G-dependent tRNA translocation on the ribosome. *Proc. Natl. Acad. Sci. U.S.A. 103*, 13670–13675.
64. Baca, O. G., Rohrbach, M. S., and Bodley, J. W. (1976) Equilibrium measurements of the interactions of guanine nucleotides with *Escherichia coli* elongation factor G and the ribosome. *Biochemistry 15*, 4570–4574.
65. Arai, N., Arai, K., and Kaziro, Y. (1977) Further studies on the interaction of the polypeptide chain elongation factor G with guanine nucleotides. *J. Biochem. (Tokyo) 82*, 687–694.
66. Pape, T., Wintermeyer, W., and Rodnina, M. V. (1998) Complete kinetic mechanism of elongation factor Tu-dependent binding of aminoacyl-tRNA to the A site of the *E. coli* ribosome. *EMBO J. 17*, 7490–7497.
67. Rodnina, M. V., Pape, T., Fricke, R., Kuhn, L., and Wintermeyer, W. (1996) Initial binding of the elongation factor Tu·GTP·aminoacyl-tRNA complex preceding codon recognition on the ribosome. *J. Biol. Chem. 271*, 646–652.
68. Stark, H., Rodnina, M. V., Wieden, H. J., Zemlin, F., Wintermeyer, W., and van Heel, M. (2002) Ribosome interactions of aminoacyl-tRNA and elongation factor Tu in the codon-recognition complex. *Nat. Struct. Biol. 9*, 849–854.
69. Valle, M., Zavialov, A., Li, W., Stagg, S. M., Sengupta, J., Nielsen, R. C., Nissen, P., Harvey, S. C., Ehrenberg, M., and Frank, J. (2003)

Incorporation of aminoacyl-tRNA into the ribosome as seen by cryo-electron microscopy. *Nat. Struct. Biol. 10*, 899–906.

70. Peske, F., Savelsbergh, A., Katunin, V. I., Rodnina, M. V., and Wintermeyer, W. (2004) Conformational changes of the small ribosomal subunit during elongation factor G-dependent tRNA-mRNA translocation. *J. Mol. Biol. 343*, 1183–1194.
71. Pfister, P., Hobbie, S., Brull, C., Corti, N., Vasella, A., Westhof, E., and Böttger, E. C. (2005) Mutagenesis of 16S rRNA C1409-G1491 base-pair differentiates between 6′OH and 6′NH_3^+ aminoglycosides. *J. Mol. Biol. 346*, 467–475.
72. Pfister, P., Jenni, S., Poehlsgaard, J., Thomas, A., Douthwaite, S., Ban, N., and Böttger, E. C. (2004) The structural basis of macrolide-ribosome binding assessed using mutagenesis of 23S rRNA positions 2058 and 2059. *J. Mol. Biol. 342*, 1569–1581.
73. Pfister, P., Corti, N., Hobbie, S., Bruell, C., Zarivach, R., Yonath, A., and Böttger, E. C. (2005) 23S rRNA base pair 2057−2611 determines ketolide susceptibility and fitness cost of the macrolide resistance mutation 2058A→G. *Proc. Natl. Acad. Sci. U.S.A. 102*, 5180–5185.
74. Battiste, J. L., Pestova, T. V., Hellen, C. U., and Wagner, G. (2000) The eIF1A solution structure reveals a large RNA-binding surface important for scanning function. *Mol. Cell 5*, 109–119.
75. Thompson, J. D., Higgins, D. G., and Gibson, T. J. (1994) CLUSTAL W: improving the sensitivity of progressive multiple sequence alignment through sequence weighting, position-specific gap penalties and weight matrix choice. *Nucleic Acids Res. 22*, 4673–4680.

BI800527K